ChemComm

COMMUNICATION

View Article Online
View Journal | View Issue

Cite this: *Chem. Commun.*, 2025, **61**, 8504

Received 31st March 2025,
Accepted 6th May 2025

DOI: 10.1039/d5cc01801c

rsc.li/chemcomm

High-contrast tricolored mechanofluorochromism of a novel gold(I)-based AIEgen achieved through the phosphino-type auxiliary ligand modulation strategy†

Zhao Chen, *[a] Yijie Zou,[a] Xiaowen Deng,[a] Xingru Liang,[a] Kaixin He[a] and Sheng Hua Liu *[b]

Two novel tetraphenylethylene-functionalized carbazole-based gold(I) complexes with phosphino-type auxiliary ligands are ingeniously designed and prepared. Significantly, this is the first time that two newly developed gold(I) complexes possessing phosphino ligands can simultaneously show aggregation-induced emission (AIE) and tricolor mechanofluorochromic properties. Furthermore, the gold(I)-bearing AIEgen with a triphenylphosphine auxiliary ligand exhibits a force-induced high-contrast three-color fluorescence switching feature.

Mechanochromic emissive materials have attracted considerable attention from researchers owing to their promising applications.[1] High-efficiency aggregate-state emission and significant difference in fluorescence colors before and after mechanical stimulation are two key indicators for achieving effective applications of mechanofluorochromic luminogens.[2] Nevertheless, most conventional luminescent materials are plagued by the notorious aggregation-caused quenching (ACQ) effect.[3] Fortunately, in 2001, Tang *et al.* put forward the aggregation-induced emission (AIE) concept, explaining the strong emission observed in the solid-state luminogens and greatly propelling the advancement of high-performance luminophores.[4] Consequently, preparing mechano-responsive emitters featuring AIE is rather significant. Thanks to the continuous efforts of scientists over the last twenty years, a number of mechanofluorochromic AIEgens exhibiting two-color fluorescence transitions have been documented.[5] For example, in 2020, Li *et al.* firstly achieved Pd^{II}-catalyzed γ-C(sp^3)–H arylation of aliphatic and benzoheteroaryl aldehydes through the synergistic use of a transient ligand and an external ligand, and two force-triggered hypsochromic two-color fluorescence switches were developed by the individual reaction of two obtained arylated intermediates and a cyano-functionalized triphenylamine derivative.[5b] In contrast, force-triggered tricolor fluorogenic molecular switches are still very rare.[6] In 2016, Ma *et al.* developed a gradually bathochromic tricolored mechanofluorochromic single crystal, whose fluorescence colors could be tuned from deep-blue to bluish-green and finally to reddish upon slight and heavy grinding.[6b] In particular, achieving force-induced hypsochromic and bathochromic bidirectional three-color fluorescence conversions of AIE-active luminogens confronts tremendous challenges.[7]

The exploitation of functionalized metal complexes is a hot research area,[8] and aurophilic interactions have attracted significant interest from scientific researchers.[9] Indeed, during the last two decades, numerous gold(I) complexes with a variety of interesting photophysical properties have been reported.[10] The development of new gold(I) complexes possessing phosphino-type ligands is an appealing research topic,[11] and some phosphino-containing gold(I) complexes with fascinating luminescence characteristics have been developed. For example, in 2022, Wang *et al.* reported a series of gold(I) luminogens bearing diverse phosphino groups, which displayed an unusual aggregation-triggered photophysical phenomenon involving the transition from thermally activated delayed fluorescence to phosphorescence.[12] Nevertheless, gold(I) complexes modified by phosphino ligands capable of exhibiting either AIE or three-color mechanofluorochromism are extremely scarce, and a phosphino ligand-based gold(I)-containing luminogenic molecule simultaneously showing both aforementioned properties has not been reported yet. The photophysical characteristics of gold(I) complexes can be effectively manipulated *via* altering the types of auxiliary ligands.[13] Therefore, simultaneously achieving AIE and tricolored mechanofluorochromism of phosphino-modified gold(I) complexes through the ligand regulating strategy is promising yet challenging.

[a] *Jiangxi Province Key Laboratory of Organic Functional Molecules, Institute of Organic Chemistry, Jiangxi Science and Technology Normal University, Nanchang 330013, P. R. China. E-mail: 1020160936@jxstnu.edu.cn*
[b] *State Key Laboratory of Green Pesticide, College of Chemistry, Central China Normal University, Wuhan 430079, P. R. China. E-mail: chshliu@mail.ccnu.edu.cn*

† Electronic supplementary information (ESI) available. See DOI: https://doi.org/10.1039/d5cc01801c

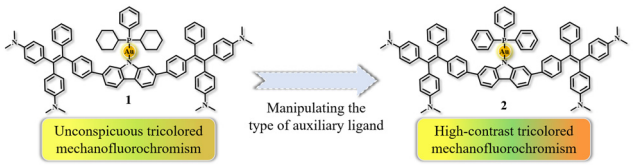

Scheme 1 Molecular structures of gold(I) complexes **1** and **2**.

In this work, two tetraphenylethylene (TPE)-modified carbazole-based gold(I) complexes with different phosphino-type auxiliary ligands were elaborately designed and synthesized (Scheme 1). The two novel mononuclear gold(I) complexes not only showed typical AIE features but also demonstrated mechanical force-induced hypsochromic and bathochromic bidirectional tricolored fluorescence switching properties, which is unprecedented for phosphino-modified gold(I) complexes. Moreover, a high-contrast three-color mechanofluorochromic phenomenon was observed for the gold(I)-based AIEgen with a triphenylphosphine auxiliary ligand, verifying the effectiveness of our ligand modulation strategy.

The synthetic routes of gold(I) complexes **1** and **2** are described in Scheme S1 (ESI†), and electrostatic potential surface maps of **1** and **2** indicated that **2** possessed more electron donor/acceptor sites (Fig. S1, ESI†).

The molecular structures of both gold(I) complexes **1** and **2** contain two TPE groups, which provide the possibility for luminogen **1** or **2** to display a remarkable AIE phenomenon.[14] AIE behaviors of TPE-modified complexes **1** and **2** were systematically studied through ultraviolet-visible (UV-Vis) absorption and photoluminescence (PL) spectroscopic techniques. The measurements in AIE investigations of **1** and **2** were performed in tetrahydrofuran (THF)-water mixed solvents with varying water fractions (f_W), conducted at a concentration of 10 μM. For the UV-Vis absorption spectra of the AIE processes of **1** and **2**, levelled-off tails in the long-wavelength region were observed with the increase of the f_W values (Fig. S2, ESI†), which was associated with the Mie scattering effect and implied the formation of nano-level aggregates.[15] As presented in Fig. S3 (ESI†), the sizes and morphologies of nano-aggregates formed by **1** and **2** in a THF–water mixture with the f_W value of 90% were visualized by scanning electron microscopy (SEM). As can be seen in Fig. 1a–d, luminogens **1** and **2** showed nearly no fluorescence in pure THF, accompanying the absolute fluorescence quantum yields (Φ_F) of 0.12% for **1** and 0.26% for **2**. When the proportion of the poor solvent water was increased to 80%, the PL of complexes **1** and **2** under 365 nm UV light became discernible, but still quite weak. Upon further increasing the f_W value to 90%, a strong emission peak was noticed with the maximum emission wavelength (λ_{max}) at 559 nm for **1** or 562 nm for **2**, and both luminogens **1** and **2** emitted high-brightness yellow fluorescence under irradiation with UV light at 365 nm. The Φ_F values of **1** and **2** in a THF–water mixture with 90% water content were measured to be 16.93% and 18.02%, respectively, which were approximately 141-fold and 69-fold higher than those in pure THF of **1** and **2**. Therefore, gold(I) complexes **1** and **2** with phosphino-type auxiliary ligands belong to the typical AIE luminogens.

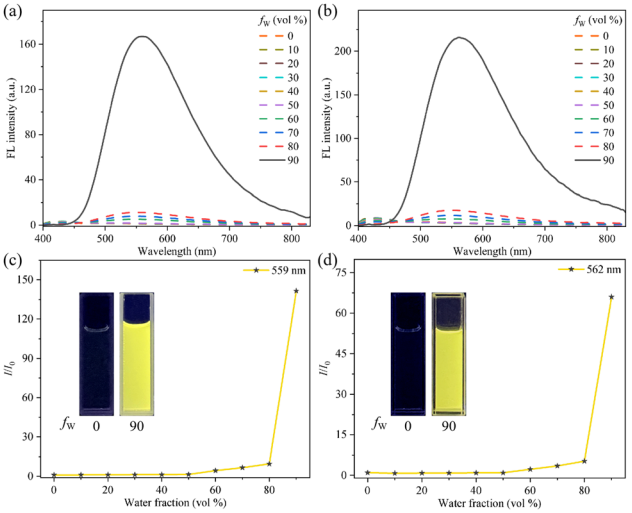

Fig. 1 Emission spectra of the dilute solutions of gold(I) complexes **1** and **2** (1.0×10^{-5} mol L^{-1}) in THF–water mixed solvents with different water contents (0–90%). Excitation wavelength = 365 nm: (a) complex **1**; (b) complex **2**. Plot of relative maximum emission peak intensity *versus* the f_W value (I = emission intensity; I_0 = emission intensity in pure THF). The insets show the PL photographs of **1** and **2** in pure THF, and 90% water content under 365 nm UV light: (c) complex **1**; (d) complex **2**.

The mechanical force-triggered fluorescence responses of luminogenic solids **1** and **2** were subsequently investigated by solid-state PL spectroscopy. As depicted in Fig. 2a–e, the PL spectrum of the pristine solid **1** showed one emission band with a λ_{max} at 551 nm, and a bright greenish yellow fluorescence was observed upon 365 nm UV illumination. After sequential slight and heavy grinding, the fluorescence color was converted into yellow-green and then to orange-yellow. Obviously, AIEgen **1** demonstrated an unconspicuous three-color mechanofluorochromism. In contrast, a force-induced hypso- and bathochromic bidirectional high-contrast tricolored mechanochromic fluorescence switching nature was noticed for AIEgen **2**. More specifically, the as-prepared sample **2** emitted a strong yellow fluorescence with a λ_{max} at 570 nm. Remarkably, gentle grinding of solid **2** using a pestle induced an evident blue shift in fluorescence emission with the λ_{max} value changing from 570 nm to 534 nm. Furthermore, upon vigorous grinding, the yellowish green fluorescence triggered by slight grinding was further converted into orange-red fluorescence with a wide-range bathochromic shift of 66 nm. Once either the heavily ground solid **1** or **2** was exposed to dichloromethane vapor for 30 s, their respective initial greenish yellow and yellow emissions from solids **1** and **2** were restored. The PL parameters of gold(I)-bearing AIEgens **1** and **2** in various solid states are summarized in Table S2 (ESI†).

To elucidate the mechanism of force-controllable three-color mechanofluorochromic phenomena exhibited by AIE-active gold(I) complexes **1** and **2** possessing phosphino-type auxiliary ligands, powder X-ray diffraction (PXRD) patterns of **1** and **2** in different solid states were measured and analyzed. As illustrated in Fig. 3, the pristine powder samples of **1** and **2** presented some strong and sharp diffraction peaks, confirming

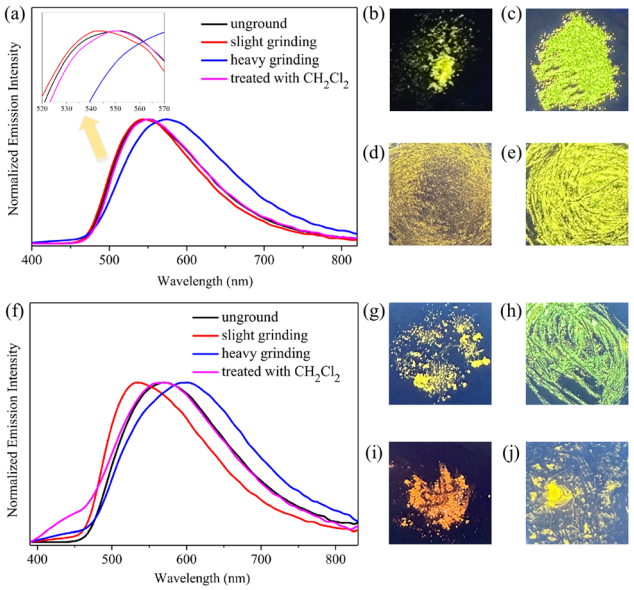

Fig. 2 PL spectra of complexes **1** and **2** in diverse solid states: (a) complex **1**; (f) complex **2**. PL photographs of complexes **1** and **2** in diverse solid states under 365 nm UV light: (b) as-synthesized solid sample of **1**; (c) slightly ground solid sample of **1**; (d) heavily ground solid sample of **1**; (e) solid sample of heavily ground solid **1** after treatment with dichloromethane; (g) as-synthesized solid sample of **2**; (h) slightly ground solid sample of **2**; (i) heavily ground solid sample of **2**; (j) solid sample of heavily ground solid **2** after treatment with dichloromethane.

their good crystalline characteristics of the as-prepared solids **1** and **2**. Upon slight grinding, some original diffraction peaks disappeared, while the intensity of the remaining diffraction peaks decreased, which implied that the initial crystallinities of solids **1** and **2** could be retained to some extent even following gentle grinding. It is possible that the synergistic effect involving loss of crystallinities, partial disruption of intermolecular forces, and conformational alterations was responsible for the hypsochromically shifted fluorescence induced by slight grinding of **1** and **2**.[16] The PXRD pattern of heavily ground solid **1** or **2** featured no visible diffraction peak, indicating the complete destruction of the well-ordered crystalline structure of the as-synthesized **1** or **2** upon vigorous grinding. Additionally, heavily ground solid samples **1** and **2** also displayed evident scattering peaks similar to those of their respective original solid states in their PXRD patterns after fumigation treatment with dichloromethane vapor, verifying their good reversibilities of mechanically responsive fluorescence behaviors of solids **1** and **2**. Reasonably, the observed tricolored mechanofluorochromic properties of **1** and **2** were attributed to mechanical force-triggered gradual transformation from well-ordered crystalline to disorderly amorphous phases, the alterations of multiple molecular packing modes, and force-controllable weakening and enhancement of intermolecular π–π interactions. Additionally, as presented in Fig. S4 (ESI†), the electron densities of the HOMO of **1** and **2** were distributed at the carbazole and two tetraphenylethylene units, and thus it was possible that the AIE properties of **1** and **2** mainly originated from the existence of two tetraphenylethylene groups. For gold(I) complex **1**, the phosphino ligand had no effect on its HOMO, HOMO−1, HOMO−2, LUMO, LUMO+1 and LUMO+2 distributions. While for gold(I) complex **2**, the electron densities of its LUMO+1 and LUMO+2 were partially distributed at the triphenylphosphine ligand. Therefore, the triphenylphosphine ligand was the key factor for achieving high-contrast three-color mechanofluorochromism of gold(I) complex **2**.

Inspired by the impressive high-contrast three-color mechanofluorochromism demonstrated by the developed AIE-active gold(I) complex **2** with a triphenylphosphine auxiliary ligand, a practical application system for ink-free writable paper was successfully constructed. As displayed in Fig. 4, the yellow fluorescent powder sample **2** was evenly spread on filter paper. Subsequently, following the pre-designed image precisely, delicate operations were carried out on the powder-coated filter paper using a thin iron rod. Specifically, specific regions were subjected to slight grinding, resulting in the formation of a defined yellowish green fluorescent pattern. Next, the other specific areas were ground vigorously, and a concrete orange-red fluorescent pattern appeared. Ultimately, a complete image consisting of a yellowish green fluorescent stem and leaf, and orange-red fluorescent sunflower was clearly visible, vividly showcasing the contrasting three-color fluorescence triggered by the mechanical force of AIEgen **2**. Notably, the formed image could be erased upon heavy grinding of the powder distributed in the stem and leaf region and subsequent dichloromethane fumigation treatment of the entire image.

In summary, two novel TPE-functionalized carbazole-based mononuclear gold(I) complexes featuring different phosphino-type auxiliary ligands were developed. It is unprecedented that two newly reported gold(I) complexes possessing phosphino ligands can simultaneously display AIE and tricolored mechanofluorochromic characteristics. Noticeably, a gold(I)-containing AIEgen **2** with the anisotropic force-triggered high-contrast three-color fluorescence switching nature was successfully

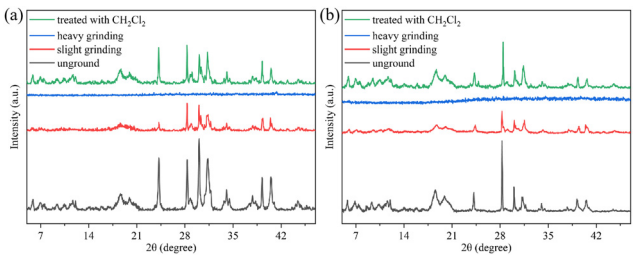

Fig. 3 PXRD patterns of complexes **1** and **2** in different solid states: (a) complex **1**; (b) complex **2**.

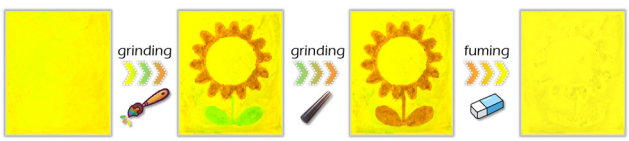

Fig. 4 Ink-free writable paper application of gold(I)-containing AIEgen **2** under 365 nm UV light.

prepared through an effective auxiliary ligand variation strategy, and luminogen **2** could achieve information storage utilizing an inkless writing approach. This work not only establishes the first successful attainment of the acquisition of AIE-active gold(I) complexes possessing phosphino ligands showing tricolored mechanofluorochromic behaviors, but also provides a reference for developing high-contrast tricolor mechanofluorochromic gold(I)-bearing AIEgens with phosphine ligands and exploring their promising applications.

We are grateful for financial support from the National Natural Science Foundation of China (22361020 and 2217 5069), the Academic and Technical Leader Plan of Jiangxi Provincial Main Disciplines (20212BCJ23004), and the Open Fund Project of Jiangxi Province Key Laboratory of Organic Functional Molecules (2024KFJJ14). This work is also supported by Jiangxi Province Key Laboratory of Organic Functional Molecules (No. 2024SSY05141).

Data availability

The authors declare that the data supporting the findings of this work are available within the manuscript and its ESI.† Should any raw data files be needed in another format they are available from the author upon reasonable request.

Conflicts of interest

There are no conflicts to declare.

Notes and references

1 (*a*) G. Yang, W.-X. Zhao, J.-Y. Cao, Z.-M. Xue, H.-T. Lin, S.-H. Chen, T. Yamato, C. Redshaw and C.-Z. Wang, *Chem. Commun.*, 2024, **60**, 3966–3969; (*b*) B. Li, A. I. M. Ali and H. Ge, *Chem*, 2020, **6**, 2591–2657; (*c*) K. Lou, Z. Hu, H. Zhang, Q. Li and X. Ji, *Adv. Funct. Mater.*, 2022, **32**, 2113274; (*d*) Z. Chen, H. Qin, Y. Yin, D. Deng, S.-Y. Qin, N. Li, K. Wang and Y. Sun, *Chem. Eur. J.*, 2023, **29**, e202203797.

2 (*a*) Q. Wan, R. Zhang, Z. Zhuang, Y. Li, Y. Huang, Z. Wang, W. Zhang, J. Hou and B. Z. Tang, *Adv. Funct. Mater.*, 2020, **30**, 2002057; (*b*) B. Prusti, S. Tripathi, P. Sivasakthi, P. K. Samanta and M. Chakravarty, *ACS Appl. Opt. Mater.*, 2023, **1**, 889–897.

3 M. Huang, R. Yu, K. Xu, S. Ye, S. Kuang, X. Zhu and Y. Wan, *Chem. Sci.*, 2016, **7**, 4485–4491.

4 (*a*) J. Luo, Z. Xie, J. W. Y. Lam, L. Cheng, H. Chen, C. Qiu, H. S. Kwok, X. Zhan, Y. Liu, D. Zhu and B. Z. Tang, *Chem. Commun.*, 2001, 1740–1741; (*b*) J. Li, J. Wang, H. Li, N. Song, D. Wang and B. Z. Tang, *Chem. Soc. Rev.*, 2020, **49**, 1144–1172; (*c*) Y. Duo, G. Luo, W. Zhang, R. Wang, G. G. Xiao, Z. Li, X. Li, M. Chen, J. Yoon and B. Z. Tang, *Chem. Soc. Rev.*, 2023, **52**, 1024–1067; (*d*) M. H. Chua, B. Y. K. Hui, K. L. O. Chin, Q. Zhu, X. Liu and J. Xu, *Mater. Chem. Front.*, 2023, **7**, 5561–5660; (*e*) X. Lyu, J. Yu, L. Zhang, Y. Zhao, Z. Qiu, Y. Chen, Z. Zhao and B. Z. Tang, *J. Mater. Chem. B*, 2023, **11**, 5953–5975.

5 (*a*) J. Zhao, Z. Chi, Y. Zhang, Z. Mao, Z. Yang, E. Ubba and Z. Chi, *J. Mater. Chem. C*, 2018, **6**, 6327–6353; (*b*) B. Li, B. Lawrence, G. Li and H. Ge, *Angew. Chem., Int. Ed.*, 2020, **59**, 3078–3082; (*c*) R. Gavale, F. Khan and R. Misra, *J. Mater. Chem. C*, 2025, **13**, 1063–1129.

6 (*a*) T. Yang, Y. Wang, X. Liu, G. Li, W. Che, D. Zhu, Z. Su and M. R. Bryce, *Chem. Commun.*, 2019, **55**, 14582; (*b*) Z. Ma, Z. Wang, X. Meng, Z. Ma, Z. Xu, Y. Ma and X. Jia, *Angew. Chem., Int. Ed.*, 2016, **55**, 519–522; (*c*) B. Zhang, J. Jiang, W. Wang, Q. Tu, R. Yu, J. Wang and M.-S. Yuan, *Mater. Chem. Front.*, 2022, **6**, 613; (*d*) S. Fu, X. Feng, N. Zhou, S. Zhang, X. Liu and D. Xu, *J. Lumin.*, 2022, **247**, 118802; (*e*) Y. Li, Z. Ma, A. Li, W. Xu, Y. Wang, H. Jiang, K. Wang, Y. Zhao and X. Jia, *ACS Appl. Mater. Interfaces*, 2017, **9**, 8910–8918; (*f*) X. Meng, G. Qi, X. Li, Z. Wang, K. Wang, B. Zou and Y. Ma, *J. Mater. Chem. C*, 2016, **4**, 7584–7588; (*g*) T. Seki, Y. Takamatsu and H. Ito, *J. Am. Chem. Soc.*, 2016, **138**, 6252–6260.

7 (*a*) Y. Yin, Q. Guan, Z. Chen, D. Deng, S. Liu, Y. Sun and S. H. Liu, *Sci. Adv.*, 2024, **10**, eadk5444; (*b*) S. Nagai, M. Yamashita, T. Tachikawa, T. Ubukata, M. Asamia and S. Ito, *J. Mater. Chem. C*, 2019, **7**, 4988–4998; (*c*) X. Wu, J. Guo, Y. Cao, J. Zhao, W. Jia, Y. Chen and D. Jia, *Chem. Sci.*, 2018, **9**, 5270; (*d*) W. Guo, M. Wang, L. Si, Y. Wang, G. Xia and H. Wang, *Chem. Sci.*, 2023, **14**, 6348; (*e*) H.-J. Kim, D. R. Whang, J. Gierschner, C. H. Lee and S. Y. Park, *Angew. Chem., Int. Ed.*, 2015, **54**, 4330–4333.

8 (*a*) L.-L. Dang, J. Zheng, D. Tian, Y.-H. Chai, T.-T. Wu, J.-X. Yang, P. Wang, Y. Zhao, F. Aznarez and L.-F. Ma, *Angew. Chem., Int. Ed.*, 2025, **64**, e202422444; (*b*) Y. Zhao, Y.-H. Chai, T. Chen, J. Zheng, T.-T. Li, F. Aznarez, L.-L. Dang and L.-F. Ma, *Chin. Chem. Lett.*, 2024, **35**, 109298; (*c*) Y. Yin, Z. Chen, R.-H. Li, F. Yi, X.-C. Liang, S.-Q. Cheng, K. Wang, Y. Sun and Y. Liu, *Inorg. Chem.*, 2022, **61**, 2883–2891.

9 (*a*) X.-Y. Wang, Y.-X. Hu, X.-F. Yang, J. Yin, Z. Chen and S. H. Liu, *Org. Lett.*, 2019, **21**, 9945–9949; (*b*) H. Schmidbaur and H. G. Raubenheimer, *Angew. Chem., Int. Ed.*, 2020, **59**, 14748–14771.

10 (*a*) Z. Li, K. Xiao, Q. Wan, R. Tang, K.-H. Low, X. Cui and C.-M. Che, *Angew. Chem., Int. Ed.*, 2022, **62**, e202216523; (*b*) A. S. Mikherdov, M. Jin and H. Ito, *Chem. Sci.*, 2023, **14**, 4485; (*c*) A. Ando, K. Ozaki, U. Shiina, E. Nagao, K. Hisano, K. Kamada and O. Tsutsumi, *Aggregate*, 2021, **3**, e125; (*d*) M. Jin and H. Ito, *J. Photoch. Photobio. C*, 2022, **51**, 100478; (*e*) S. Cheng, Z. Chen, Y. Yin, Y. Sun and S. Liu, *Chin. Chem. Lett.*, 2021, **32**, 3718–3732; (*f*) H. Amouri, *Chem. Rev.*, 2023, **123**, 230–270.

11 (*a*) J. J. Mihaly, S. M. Wolf, A. T. Phillips, S. Mam, Z. Yung, J. E. Haley, M. Zeller, K. de, L. Harpe, E. Holt, T. A. Grusenmeyer, S. Collins and T. G. Gray, *Inorg. Chem.*, 2022, **61**, 1228–1235; (*b*) M. Pujadas and L. Rodríguez, *Coord. Chem. Rev.*, 2020, **408**, 213179.

12 X.-Y. Wang, J. Gong, H. Zou, S. H. Liu and J. Zhang, *Aggregate*, 2022, **4**, e252.

13 (*a*) X. Deng, S. Liu, C. Fan, H. Liu, Y. Zou, H. He, D. Deng, S. Pu and Z. Chen, *Spectrochim. Acta. A*, 2024, **321**, 124712; (*b*) H. Beucher, J. Schörgenhumer, E. Merino and C. Nevado, *Chem. Sci.*, 2021, **12**, 15084–15089; (*c*) I. Soldevilla, A. G. El-Hachimi, R. Ramazanov, R. R. Valiev, M. E. Olmos, M. Monge, D. Sundholm, M. Rodríguez-Castillo and J. M. López-de-Luzuriaga, *J. Mater. Chem. C*, 2024, **12**, 13255–13267.

14 (*a*) G. Yashwantrao, M. Debnath, A. Gavali, S. Seth, P. Badani, R. Srivastava and S. Saha, *Dyes Pigments*, 2025, **232**, 112462; (*b*) P. Q. Nhien, H.-K. Chang, T. T. K. Cuc, T. M. Khang, C.-H. Wu, B. T. B. Hue, J. I. Wu and H.-C. Lin, *Sens. Actuators, B*, 2022, **372**, 132634.

15 J. Liang, Z. Chen, J. Yin, G.-A. Yu and S. H. Liu, *Chem. Commun.*, 2013, **49**, 3567–3569.

16 P. S. Hariharan, V. K. Prasad, S. Nandi, A. Anoop, D. Moon and S. P. Anthony, *Cryst. Growth Des.*, 2017, **17**, 146–155.